# Nanoscale

Accepted Manuscript


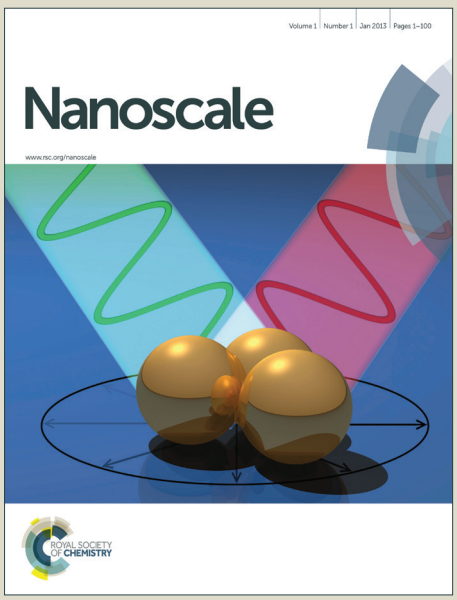





ROYAL SOCIETY OF CHEMISTRY

www.rsc.org/nanoscale

Nanoscale

ARTICLE

# Upconversion luminescence behavior of single nanoparticles

Jiajia Zhou[a], Shiqing Xu[a,*], Junjie Zhang[a], Jianrong Qiu[b,*]

Received 00th January 20xx,
Accepted 00th January 20xx

DOI: 10.1039/x0xx00000x

www.rsc.org/

Upconversion nanoparticles (UCNPs) have made a significant and valuable contribution to materials science, photophysics, and biomedicine, due to their specific spectroscopic characteristics. However, the ensemble spectroscopy of UCNPs is limited for the electronic behavior in average effect, which ignores the fact that the nanoparticles are heterogeneou . Towards the research focus of heterogeneous intrinsic structure, unique photophysical phenomena, and advanced applications, the optical characterization of single UCNPs are promoted to a frontier breakthrough of UCNPs communit . In this review, we overview the importance of the single UCNPs characterization, the typical principles of UC, and the single particle detection methods. A considerable emphasis is placed on the specific spectroscopic study of single UC which shows us fantastic photophysical phenomena beyond ensemble measurement. Parallel efforts are devoted to th current applications of single UCNPs.

## Introduction

Upconversion (UC) luminescence from lanthanides doped nanoparticles with unique spectroscopic conversion ability has become a fast-developing research field in recent years, which exhibits different kinds of promising applications in biomedicine, photovoltaic, 3D display, sensing, *etc.* This photon management in nanoscale has superiority in optical tunability including the aspects of excited-state dynamics, emission spectra, quantum efficiency, *etc.* For instance, near-infrared (NIR) excited multicolor UC could be applied in multiplexed labeling through the control of dopant species, concentration, and their spatial distribution. Single-band red or NIR UC emission with high productivity is very promising for deep *in vivo* imaging and cell tracking. Composite composed of UC nanoparticles and semiconductors ($TiO_2$, ZnO, *etc.*) has spectral conversion characteristic from NIR to UV for solar energy harvest in photovoltaic or photocatalysis.

One will easily find that all of these prevalent researches on UC nanoparticles (UCNPs) are focus on their optical performance by ensemble spectroscopy techniques. Little efforts have been contributed to the single nanoparticle UC luminescence behavior, though it's well known that with the knowledge gained through single particle spectroscopy, the performance of the UC particles could be optimized.

UCNPs, *e.g.* $NaYF_4$, which is considered as a typical representative, have an average size ranging from sub-20 n to 100 nm. Most of the UCNPs are synthesized by wet chemical methods, and are expected to disperse in variou kinds of solvents to form a colloid. In addition, the surfac functionalization of UCNPs is an extremely important proc in bio-applications. For instance, the significant proportion of atoms lying around the surface, combined with the enriched surface defects and organic ligands, can significantly complicate the photophysical behaviors of the dope lanthanides. The electronic behavior detection aiming at a single nanoparticle will show signals from the micro-structur of nanoparticles. Moreover the single nanoparticle spectroscopy offers clear insight into the interplay betwee intrinsic and extrinsic influences without noise, and subsequently gives instructions for the high qua preparation of UCNPs.

On the other hand, single nanoparticle optical characterization possesses a powerful capacity to explore th crystalline structure anisotropy related optical differences, o some unexpected unique optical phenomena at sub-mic and even nano-scale. For instance, earlier developed artifici nano materials, quantum dots and metal nanoparticles hav been widely investigated in single nanoparticle photophysic For example, the first reports of the detection of single CdS nanocrystals revealed a number of novel photophysica phenomena that had not been expected. $NaYF_4$, or any othe UCNPs with isolated activators, which are different from th conductor or semiconductor on luminescent principle, ar expected to be discovered new photophysical phenomena From photophysical theoretical investigations to singl nanoparticle technical applications, single UCNPs focused optical characterization plays an important role in optica super resolution imaging, local field enhanced luminescence *etc.*

[a] College of Materials Science and Engineering, China Jiliang University, Hangzhou 310018, China. E-mail: shiqingxu75@163.com
[b] State Key Laboratory of Silicon Materials, School of Materials Science and Engineering, Zhejiang University, Hangzhou 310027, China. E-mail: qjr@zju.edu.cn

In this paper, we present the first short review on the UC behaviors of single UCNPs spanning from the typical UC principles, single particle spectroscopic detection technology, to the recent developed new photophysical phenomena and applications in single particle level.

## Principles of upconversion luminescence

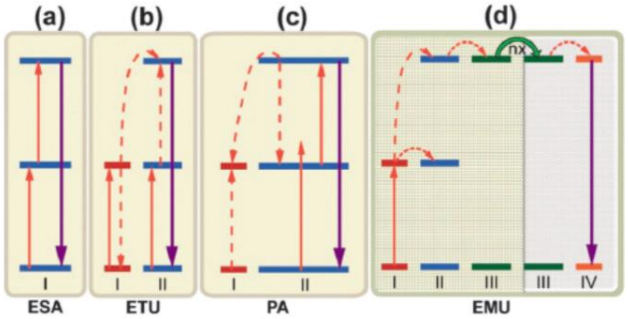


**Figure 1** Proposed typical UC processes: (a) Excited state absorption (ESA); (b) energy transfer UC (ETU); (c) photon avalanche (PA). (d) energy migration-mediated UC (EMU) involving the use of four types of lanthanide ions and a core-shell design[1]

Upconversion is an Anti-Stokes process, which converts two or more low-energy photons into one high-energy photon. The occurrence of this phenomenon benefits from the relative long lifetime of most of the excited states in trivalent lanthanides. UC luminescence has been attracted unprecedented attention referring to various promising applications including photovoltaic, bioimaging, solid-state laser diode, temperature sensor, lighting, *etc.*, since the UC has been firstly observed by Auzel in 1960s.

The higher prevalence and practicability of UC compared to multi-photon absorption and second/third harmonic generation are contributed by the relatively low excitation energy and high quantum efficiency. In general, the UC occur in four different ways (Figure 1). Figure 1(a) illustrates the excited state absorption (ESA), where sequential absorption of two photons occurs and the ion is exited to higher state via a real intermediate state. Figure 1(b) shows the energy transfer UC (ETU), which means two neighboring ions are excited to the intermediary states by ground state absorption followed by non-radiative energy transfer between the two ions. Figure 1(c) presents the photon avalanche (PA). This is an unconventional process, where the strong UC luminescence occurs without the resonance ground state absorption when the excitation power exceeds a certain threshold. The pump wavelength is only resonant between a metastable state and a higher energy state. The energy migration-mediated UC (EMU) in Figure 1(d) is recently proposed by Wang et al.[2], involving the use of four types of lanthanide ions and a core-shell structure. The ions without long-lived intermediary energy states ($Ln^{3+}$= $Eu^{3+}$, $Tb^{3+}$, $Dy^{3+}$, $Sm^{3+}$) become activators to generate efficient UC luminescence in $NaGdF_4$:$Tm^{3+}$/$Yb^{3+}$@$NaGdF_4$:$Ln^{3+}$ core-shell nanoparticles benefitting from the energy migration effect of $Gd^{3+}$ located in the host lattice.

## Detection approaches for single particle spectroscopy

Detection of single UCNPs is an advanced technique with the requirement of background knowledge in material science and optical engineering. In all detection approaches, high resolution microscopes, overcoming the light diffraction limit, constitutes the main components. In general, the 980 nm laser source is employed to excitation and selected ultraviolet, visible or NIR wavelength regions are detected. So far, two mainstream approaches are mainly used for single UCNPs optical characterization: confocal scanning microscopy and fiber loaded measurement. They stand out from the other methods, *e.g.,* photonic force microscopy, fiber tapper measurement. In this part, we will give a brief introduction of the key techniques in these two approaches.

**Confocal scanning microscopy** Confocal scanning microscopy possesses the advantage of high signal-to-noise ratio with the spatial filtering effect compared to wide-field microscopy. In this scheme, the out-of-focus signals do not pass the hole and are not detected by the detector, as is shown by the grey dot lines in Figure 2. In a typical single nanoparticle upconversion measurement[3-9], a 980 nm diode laser is tightly focused on the sample through an objective. The sample is raster scanned by a piezo-actuated three-dimensional nanopositioning stage. At each pixel, the UC luminescence is collected through the same objective, and passed through a dichroic beam splitter and short-pass filters, while the 980 nm excitation light is completely filtered out. After passing through a confocal pinhole, the upconversion luminescence is either detected by a spectrometer for spectrum collection or an avalanche photo diode (APD) for luminescence image acquisition.

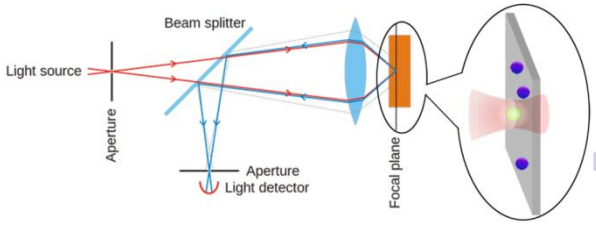


**Figure 2** Schematic diagram of confocal scanning microscopy

In the confocal scanning microscopy, single nanoparticle hunting is time consuming, which makes the sample preparation a skill demanding work, though the atomic force microscope (AFM) is usually in situ combined to the optical detection[4, 5]. Empirical methods contain the TEM grids loading and coverslip loading through dropping process of diluted nanoparticle solution with concentration of ~0.1 nM. Using the TEM grids, the single particles could be further confirmed by the TEM or SEM imaging. Note that this should be carried out after all optical characterization to avoid perturbing the optical properties caused by high-energy electrons. For the coverslip approach, it is indeed a tricky task to obtain monodisperse particles in appropriate distribution for single detection. In this case the employment of surface treatment agent on top of the coverslip may be helpful. Besides, to avoid agglomeration of the nanoparticles during evaporation of the solvent,

coverslip itself could be stored on a support mount on a beaker in an ultrasonic bath.

**Fiber loaded measurement** Luminescence detection using liquid-immersed exposed-core microstructured optical fibers (MOF) has been frequently reported by Monro et al.[10-12] . Recently, the single-nanocrystal sensitivity has been achieved by enhanced UC luminescence, which results from the cooperation of Jin's group and Monro's group. This makes the fiber loaded technology to be a powerful approach for single UCNPs detection[13, 14] . The schematic of the experimental configuration for capturing UC luminescence of nanoparticles using a suspended-core microstructured optical-fiber dip sensor is demonstrated in Figure 3. A 980 nm fiber-coupled diode laser source is used for excitation. It's coupled into the MOF using a dichroic mirror and a microscope objective. The UC emission is collected by the same fiber core and propagates backward direction to the excitation light. After the fiber light propagates through the dichroic filter and a broad band-pass filter where residual back scattered pump light is removed, and the particle luminescence is detected by a spectrometer. The experimental procedure firstly involves optimizing and recording the amount of power coupled into the suspended core of the fiber by varying the fiber position using XYZ stages. The lens is then removed from the output coupling stage, and the tip of the fiber immersed in the nanoparticle solution where fiber holes are filled with solution due to capillary forces. The fiber is then removed from the solution and the measurement is performed. Here the nanoparticle solution is diluted UCNPs dispersed in a nonpolar solvent, *e.g.*, toluene, cyclohexane, *etc.*, with a concentration ranging from tens of fM to tens of nM.

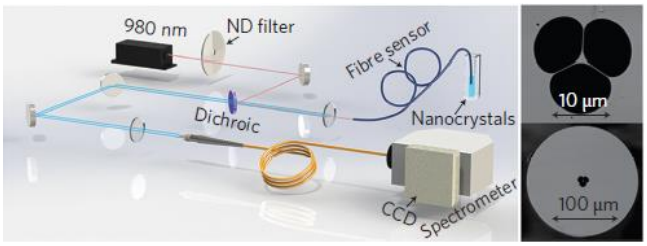


**Figure 3** Schematic of the experimental configuration for capturing UC luminescence of nanoparticles using a suspended-core microstructured optical-fiber dip sensor[13]

## Specific spectroscopic study of single UCNPs beyond ensemble spectroscopy

Single particle characterization is a powerful technical approach to exploit the microstructural dependent spectroscopic characters, which is always compromised in ensemble spectroscopy. For instance, both of the "bright" and "dark" spots representing the UC efficiency of different hexagonal $NaYF_4$ may coexist in an imaging field. It's a clear signal that some unknown defects may be induced in the synthesis to generate inconsistent crystalline symmetries between particles though they have similar morphologies; or the different particles lying with different lattice planes on surface, which may have specific atomic density and orientation effects with polarized laser beam. This kind of precise spectroscopic study is of great importance to improve the quality of UCNPs, but it's ignored in ensemble measurements. Here we would like to introduce some important fundamental developments devoted to the upconversion luminescence behaviors of single nanoparticles.

**Non-blinking and non-bleaching luminescence** Photoluminescence blinking—random switching between states of high (ON) and low (OFF) emissivities—is a universal property of molecular emitters found in single quantum dots and fluorophores[15-17] . Also, the observed time scale of blinking ranges from several hundred milliseconds to several seconds of single $Eu^{3+}$ ions incorporated in $Y_2O_3$ nanoparticles[18] . However, such behavior is absent in single nanoparticles with abundant lanthanides. For the lanthanides activated UCNPs, the question—blink or not—has been confirmed by single particle characterization using confocal or wide field microscopy[3, 9, 19] . As it is displayed in Figure 4, the first graphical demonstration of non-blinking behavior and photobleaching or photodamage after 1 h of continuous laser illumination was reported by Cohen et al. in single (β-$NaYF_4$) nanoparticles doped with 20% $Yb^{3+}$and 2% $Er^{3+}$, which subsequently is considered to be ideally suited for single molecule imaging. Since then, the way that to do the upconversion intensity fluctuation assessment of a laser focused single particle over a considerable period of time has been frequently used to confirm the photostability of UCNPs. This is practically considered as a prerequisite of UCNPs from materials science for the feasibility in biomedical science. Such successful examples are listed in Table 1. Moreover, single particle imaging with spectral exhibition is used to accurate assessment of the brightness of UCNPs with different micro-structures[20] .

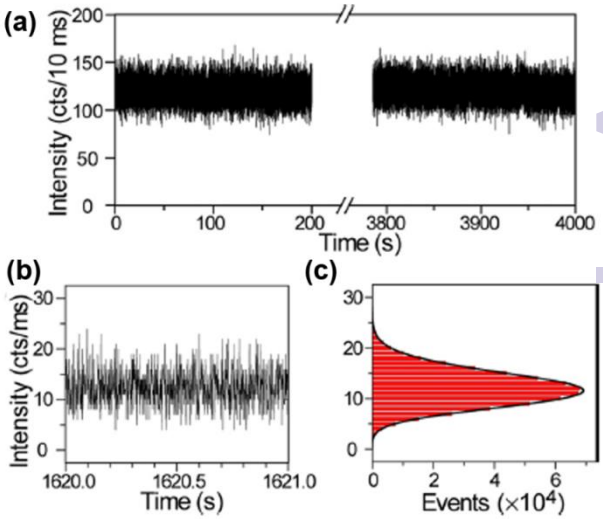


**Figure 4** Photostability and non-blinking behavior of a single UC nanoparticle. (a) The time trace of emission intensity from a single UC nanoparticle under continuous laser illumination for more than 1 h. (b,c) The zoom-in time trace and histogram of emission intensity, showing no on/off behavior -non-blinking[3]

Nanoscale

ARTICLE

**Table 1** Photostability and brightness assessment of single UCNPs

| UCNPs | Particle size (nm) | Monitoring wavelength (nm) | Assessing mode | Power density ($W \cdot cm^{-2}$) | Time range (min) | Ref. |
|---|---|---|---|---|---|---|
| β-$NaYF_4$: $Yb^{3+}$,$Er^{3+}$ | ~27 | 550/650 | photostability | $5 \times 10^6$ | 60 | 3 |
| $NaGdF_4$:$Yb^{3+}$,$Er^{3+}$@$NaGdF_4$ | ~40 | 550/650 | photostability | 150 | 240 | 19 |
| $YVO_4$:$Yb^{3+}$,$Er^{3+}$ | ~39 | 520/550/650 | photostability | $8 \times 10^3$ | 8 | 21 |
| $NaYF_4$ :$Yb^{3+}$,$Ho^{3+}$,$Tm^{3+}$@$NaYF_4$ | ~22 | 450/475/545/645 | photostability | $8 \times 10^6$ | 360 | 22 |
| β-$NaYF_4$: $Yb^{3+}$/$Er^{3+}$ | ~10 | 550/650 | photostability | $10^6$ | 60 | 9 |
| β-$NaGdF_4$:$Yb^{3+}$,$Er^{3+}$@$NaYF_4$ | ~20 | 520/550/650 | brightness | / | / | 20 |
| β-$NaGdF_4$:$Yb^{3+}$,$Er^{3+}$@$NaGdF_4$ @$SiO_2$@NPTAT-doped $SiO_2$ | ~39 | 550 | photostability | / | 15 | 23 |
| β-$NaGdF_4$:$Yb^{3+}$,$Tm^{3+}$@$NaGdF_4$ @$SiO_2$@NPTAT-doped $SiO_2$ | ~38 | 480 | | | | |
| $NaYbF_4$:$Er^{3+}$@$NaYF_4$@$SiO_2$@rhodamine B isothiocyanate-doped $SiO_2$ | ~24 | 650 | | | | |

**Polarization anisotropic upconversion** Micro-polarized spectroscopy that focuses on the single particle luminescence has attracted great attention in semiconductor system. In contrast to single emission bands observed for semiconductor system, the lanthanides-doped UCNPs generally show a distinct set of sharp emission peaks arising from f–f orbital electronic transitions. The multiple-peak patterns should provide spectroscopic fingerprints, which are particularly useful for accurate interpretation in the event of overlapping emission spectra, thus possibly make themselves to detailed theoretical analysis. What's more, UC with the requirement of laser excitation will be affected by the polarization state spontaneously. However, it's still an open question whether the nanoparticles with abundant activators should exhibit polarization anisotropy under linearly polarized laser excitation, though the single lanthanide ion transitions have polarization orientation. Therefore, we tried to demonstrate micro-polarized optical detection of UC based on lanthanides doped inorganic dielectric system, namely, $Tm^{3+}$-$Yb^{3+}$ ion couple activated β-$NaYF_4$ single microrod for the first time[6]. During this single particle detection, unique luminescent phenomena have been observed upon excitation with 980 nm linearly polarized laser, *e.g.* sharp energy level split and singlet to triplet transitions at room temperature, multiple discrete fluorescence intensity periodic variation with polarized direction (Figure 5 (a-d)). The comparative experiments suggested that intra-ions transition orientation and crystal local symmetry dominate the polarization anisotropy. In purpose of the origin exploration of polarization anisotropy with convincing experimental design, we further employed the excitation polarization detection considering of the interplay between the azimuth of laser polarization and the crystallography axis[24]. As it is shown in Figure 5 (i, k), the linearly polarized laser beam was focused onto two nanodisks with face up (i) and side up (k), and the excitation polarization angle was defined to be 0° when the laser is polarized parallel to the a axis or c axis, respectively. For the side up particle, it was observed that the UC luminescence intensity changes periodically when the polarization angle of excitation light is changed from 0° to 360°. And the polarization degree is as large as 0.78, 0.79, and 0.74 for the $^2H_{11/2} \rightarrow {}^4I_{15/2}$, $^4S_{3/2} \rightarrow {}^4I_{15/2}$ and $^4F_{9/2} \rightarrow {}^4I_{15/2}$ transitions of $Er^{3+}$. However, this UC luminescence dependence on excitation polarization could be ignored in the case of the face up particles. This measurement proved useful information that the polarization of UC luminescence depends upon the orientation of the nanodisk with respect to the polarization angle of the excitation light or the detection.

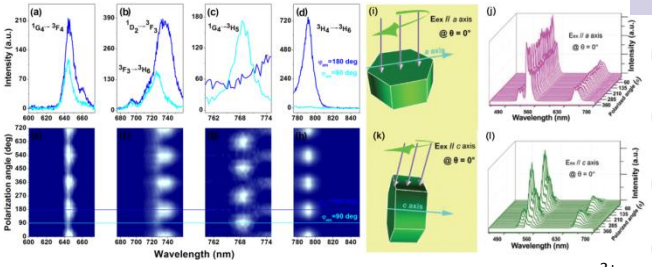


**Figure 5** (a-d)Emission spectra of UC from β-$NaYF_4$: $Tm^{3+}$-$Yb^{3+}$ single micro-rod in the transitions of $Tm^{3+}$: (a) $^1G_4 \rightarrow {}^3F_4$, (b) $^3F_3 \rightarrow {}^3H_6$, $^1D_2 \rightarrow {}^3F_3$,(c) $^1G_4 \rightarrow {}^3H_5$, (d) $^3H_4 \rightarrow {}^3H_6$, respectively.(e–h) show the dependence of the corresponding spectra on the emission polarization angle ($\varphi_{em}$). (i, k) Schematic representation of the $NaYF_4$nanodisk with its a axis (i) or c axis (k) parallel to the horizontal plane (HP). (j, l) UC luminescence

spectra of a single nanodisk, whose a axis (j) or c axis (l) is parallel to HP, recorded at excitation polarization angles varying from 0° to 360°, with no polarizer placed in the detection part.[6, 24]

**Concentration quenching abatement** Dopant concentration is a crucial factor to determine the UC brightness and color display[25, 26] . Strong absorption, critical distance between donor and acceptor, and radiative efficiency are concentration dependent. High dopant concentrations have been found to result in quenching of the luminescence due to cross-relaxation. Therefore, optimum dopant concentration to avoid quenching is frequently emphasized in most studies, *e.g.,* the optimal $Tm^{3+}$ concentration in the upconverted $NaYF_4$ host lattices has been found in the range of ~0.2-0.5 mol% at excitation irradiance below 100 $W{\cdot}cm^{-2}$ (with ~20-40 mol% $Yb^{3+}$)[27-31] . Recently, Zhao *et al.* presented evidence that UC luminescence can be significantly enhanced by using much higher activator concentrations under relatively high-irradiance excitation[13] . In other words, the concentration quenching or UC saturation threshold value could be greatly increased in single nanoparticle with high power excitation. As is shown in Figure 6(a), increasing the excitation irradiance from $1.6{\times}10^4$ $W{\cdot}cm^{-2}$ to $2.5{\times}10^6$ $W{\cdot}cm^{-2}$ enhances the overall UC luminescence intensity by factors of 5.6, 71 and 1105 for 0.5 mol%, 4 mol% and 8 mol% $Tm^{3+}$ concentrations, respectively. Importantly, at high excitation and high $Tm^{3+}$ doping level, the fraction of excitation energy producing UC emission is increased. This demonstrates that UC is more efficient at high excitation and for high $Tm^{3+}$doping. Similarly, Gargas *et al.* also reported that the extra UC yield could be produced with high concentration and high excitation irradiance in the case of 20 mol% $Yb^{3+}$-20 mol% $Er^{3+}$ couple[7] . And the fascinating single particle luminescence images with low, medial, and high laser intensity give a clear evidence of this concentration quenching abatement effect of single nanoparticles with high doping (Figure 6(b)).

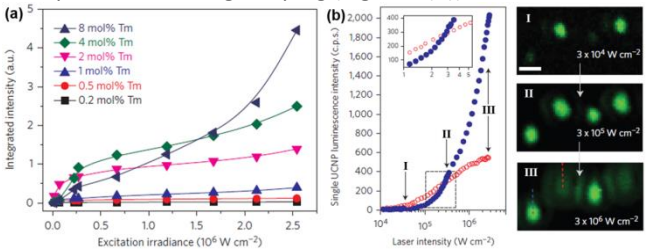


**Figure 6** Luminescence intensity of single UCNPs as a function of doping concentration and laser intensity. (a) Integrated UC luminescence intensity (~400-850 nm) as a function of excitation irradiance for a series of $Tm^{3+}$-doped nanoparticles. (b) Luminescence intensity of single 8 nm UCNPs with 20% (blue circles) and 2% (red circles) $Er^{3+}$, each with 20%$Yb^{3+}$, plotted as a function of excitation intensity. Confocal luminescence images taken at points shown in (b) of single UCNPs containing a mixture of 2% and 20% $Er^{3+}$[7, 13]

**Intense multiphoton upconversion** Multiphoton UC with large Anti-Stokes shift is produced to potential applications including photocatalysis, super-resolution imaging, *etc.* $Tm^{3+}$, as the most popular activator to generate multiphoton UC, has perfect ladder-type electron configuration with fairly sm… mismatch in relation to the energy feeding from $Yb^{3+}$ step-by… step. The concentration of the classic combination for $Tm^{3}$… $Yb^{3+}$ couple is about 2 mol%-20 mol% in hexagonal $NaYF_4$ hos… which is found for the utilization of the strong 2-photon nea… infrared (NIR) emission[32] . Actually, the lower the… concentration of $Tm^{3+}$, the higher the multiphoton U… percentage will be obtained on account of the avoidance of… cross relaxation quenching. However, one should note tha… this energy distribution status of multi- and 2-photons… populations shown in the spectrum is at the cost of the overall… quantum efficiency of UC, due to the small activator number… Benefiting from the saturation excitation effect in singl… nanoparticle mode, we successfully observed the luminescen… switching between the emissions from 2-photon UC and multi… photon UC at 2 mol % $Tm^{3+}$-20 mol % $Yb^{3+}$ with the increasing… of laser power (Figure 7 (a,b)). The achievement of the su… intense multiphoton UC of $Tm^{3+}$ — specifically, the emission… intensity of blue 4-photon UC exhibits an increase by a fac… of ~ 70 in comparison with the NIR 2-photon UC under 980 nm excitation (Figure 7 (c)) — may promote the $Yb^{3+}$-$Tm^{3+}$… couple to be a good candidate of lanthanide activator for NI… excited super-resolution UC imaging.

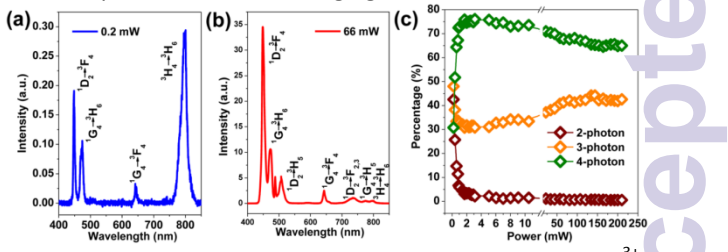


**Figure 7** (a, b) Emission spectra of single β-$NaYF_4$: 20 $Yb^{3+}$-2… $Tm^{3+}$ nanoparticle excited with 980 nm laser illumination a… the power of 0.2 mW (~$3.5{\times}10^4$ $W{\cdot}cm^{-2}$) and 66 mW… (~$1.1{\times}10^7$ $W{\cdot}cm^{-2}$), respectively. (c) Laser power dependent… multiphoton UC radiative percentages in the wavelength ra… from 400 nm to 850 nm of single□β-$NaYF_4$: 20 $Yb^{3+}$-2 $Tm^{3+}$nanoparticle[33]

**Heterogeneous emission profiles** Nanoparticles, which are… synthesized by wet-chemical methods with different kinds of… surfactants, are usually capped with corresponding surfac… chemical bonding. For example, all of the three conventional… ways (coprecipitation, thermal decomposition, an… solvothermal ways) used to synthesize $NaYF_4$ UCNPs cause the… introduction of oleic acid molecules or oleic acid ions ligand… attaching to the surface of the particles[2] . These surface ligands… accompany with the crystal defects will affect the precisio… spectroscopy of each nanoparticles. From the precision… spectral investigation particle-by-particle, the microscop… electron behavior and energy transfer mechanism explorati… would be certainly improved; more importantly, it make… sense to obtain high efficient UCNPs by intrinsic improvement… A pioneering discovery has been reported by Gargas *et a…* typical heterogeneous high-resolution spectra are shown…

Figure 8, with particle-to-particle variations in peak intensities at 541 and 557 nm. The addition of undoped $NaYF_4$ shells to these nanoparticles eliminates this heterogeneity (Figure 8, bottom trace) suggesting a region within the nanoparticles in which the lanthanides may be emissive but are energetically coupled to the surface. The observed spectral differences may arise from either variation in lanthanide distributions between nanoparticles, or from subtle variations in surface defects, surface reconstruction, or faceting. This identification of losses from energy transfer to the surface suggests one means for improving emission from nanoparticles.

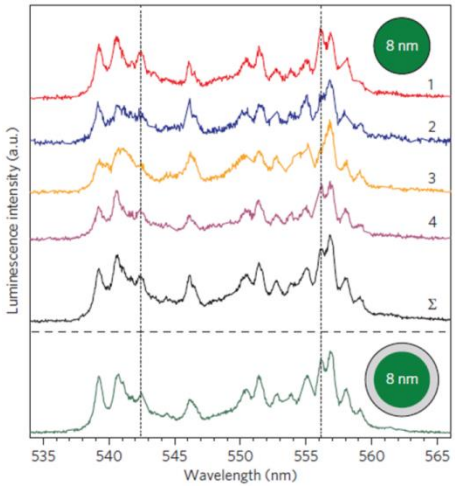


**Figure 8** Fine spectra of thegreen emission bands collected from four single 8 nm UCNPs (curves 1–4)and their averaged spectra (curve Σ). Vertical dotted lines highlight peaks exhibiting heterogeneity between individual UCNPs. The green emission spectrum of an 8 nm UC nanoparticle with epitaxial 1.8 nm undoped shell is shown below the horizontal dashed line.

**Lifetime-tunable imaging** Lifetime is another dominant characteristic besides of the emission profile with fingerprint effect of Lanthanides' electronic transitions. Lanthanides have their 4f-4f transitions in a time range from microseconds to milliseconds. Among typical materials that emit such long-lived luminescence, lanthanides doped UCNPs are attracting significant attention with their application in sensing, bioimaging, and 3D display. Although it's widely known that the lifetime of lanthanides could be tuned by their concentration in a local environment, the issue of how best to control and fine tune the lifetimes that cover a broad temporal range targeting to certain application is a challenge. Recently, Lu et al. developed more than ten nanocrystal populations with distinct lifetimes ranging from 25.6 μs to 662.4 μs and decoded their well-separated lifetime identities in single color band. This precisely tuning of lifetime has been vividly demonstrated in a single nanocrystal's emission at 475 nm[34]. Figure 9 shows confocal images of five typical groups of lifetime-encoded Tm-doped 'τ-dots', using pseudocolour to map the luminescence lifetime for each pixel. This is a pioneering discovery of single nanoparticle characterization that focuses on transient state of electronic transition rather than steady state. The multi-dimensional comprehensions and views of upconversion behavior are promising for further advance the broad application prospect of UCNPs.

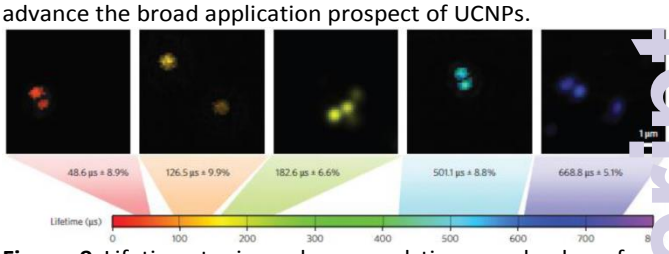


**Figure 9** Lifetime tuning scheme and time-resolved confocal images for $NaYF_4$: Yb, Tm upconversion nanocrystals[34]

## Applications in single UCNPs level

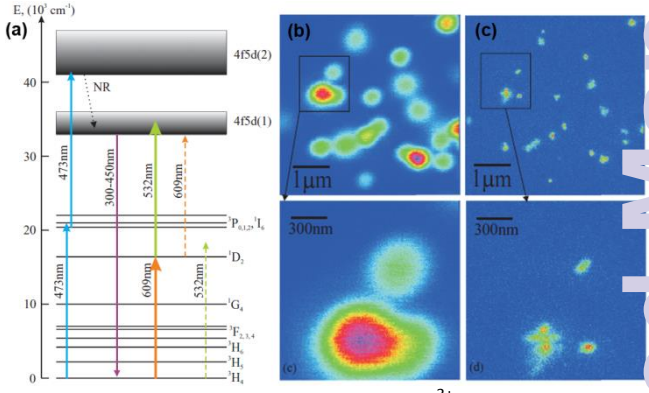


**Figure 10** (a) Energy level diagram of $Pr^{3+}$ electronicstates in YAG crystal. (b) Confocal image of $Pr^{3+}$: YAG nanoparticles.(c) Super-resolution image of the same area[35]

**Super-resolution upconversion imaging** Upconversion is of high interest for microscopy because of the excellent imaging quality without luminescence background. The combination of the advantages of super-resolution optical microscopy techniques and the UCNPs is an advanced exploration with significant importance. In terms of the fluorescent species dependent super-resolution technique, a breakthrough of optical resolution could be achieved by using UCNPs. Simultaneously, for the widespread research on lanthanides doped UCNPs spanning from chemosynthesis, dynamical model, spectroscopic analysis, and ensemble application, it's a frontier development in single particle level to realize super-resolution UC imaging. Up to now, the reported feasible solution is a method which resembles stimulated emission depletion microscopy (STED) involving stimulated absorption rather than stimulated emission. In this method, a three-level system and long-lived intermediary state are necessary, *e.g.,* $Pr^{3+}$: $^3H_4$-$^1D_2$-4f5d system with long lifetime of $^1D_2$ (150-200□s) was used by Kolesov *et al.*[35]. As is shown in Figure 10(a) the $^1D_2$ level is excited by an orange 609 nm laser, and a donut-shaped 532 nm beam is exploited as a second excitation step. In that situation, the population of $^1D_2$ level will be depleted by the donut green beam unless the particle is not in the very center of the donut. After that, the remaining population of $^1D_2$ state can be read out by a short 532 nm pulse. Finally, comparing with the confocal images (Figure 10(b)) and the super-resolution images (Figure 10(c)), the

optical resolution value can be improved by at least an order of magnitude. This best resolution obtained so far was~50 nm and is limited by the size of nanoparticles. Further improvement is expected to be realized using $NaYF_4$:$Yb^{3+}$-$Tm^{3+}$ UC system with smaller particle size.

**Location control investigation of luminescence enhancement** Plasmonic local field effect on luminescence is a controversial topic because of the vague theoretical origin of enhancement and the random occurrence of enhancement or quenching[36-38]. One recognized experience from the previous research is that the positional relation between emitters and the metallic surfaces or particles possess a critical importance on the field effect[39]. The investigation to this point has been successfully performed with controllable nanoassembly of UCNPs and gold nanospheres in single particle mode, and even with the consideration of the laser polarization effect[5]. As is shown in Figure 11 (a), the gold sphere was brought in the vicinity of the UC nanoparticle with their central axis along the laser polarization axis. The non-equative rates of increase between green and red emission by a factor of 4.8 and 2.7 have been observed from the UC spectra in Figure 11 (b). The plasmonic enhancement effect on the emission of the nanoparticle was also reflected in a reduction of the rise and decay times (see Figure 11 (c)). This controlled study of UC using single nanoparticle accurate characterization will provide important input for the optimum design of future hybrid UCNPs and metal nanostructures.

Similarly, tip-enhanced luminescence is an effect that the locally enhanced electric fields in the vicinity of a sharp metal tip to amplify the excitation and emission rates in a nearby sample object. Very recently, Mauser *et al*. presented the first near-field study of a single $NaYF_4$ nanoparticle doped with $Yb^{3+}$-$Er^{3+}$ using an AFM scanning tip[40]. The strong UC luminescence amplification (Figure 11(e)) indicated the tip-enhanced near-field effect, and the enhancement factor was in general agreement with the near-field to far-field ratios calculated according to the experimental configuration (Figure 11(d)). The significantly faster decay of the lifetime in the presence of the tip (Figure 11(g)) and tip-sample distance curves confirmed the contribution of radiative rate enhancement. This study indicates the penitential of this single nanoparticle technique for the characterization of more complex upconverting structures with subtle target, *e.g.,* to demonstrate the lattice plane sensitive enhancement in a single hexagonal particle.

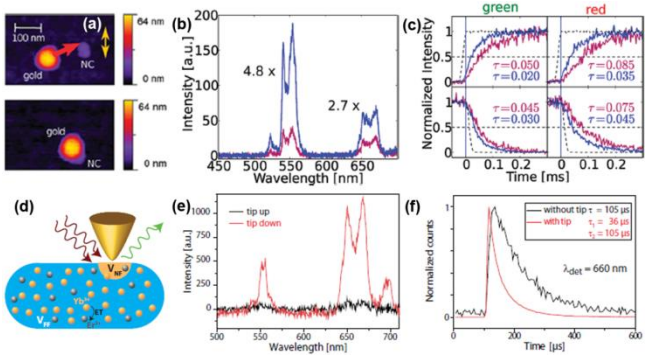


**Figure 11** (a) AFM image showing the nanoassembly approach: The 60 nm gold nanosphere is attached to the NC with the help of the AFM tip. The yellow arrow indicates the polarization axis of the excitation light. (b) UC emission spectra of the nanoparticle without (violet curve) and with (blue curve) the gold nanosphere in close vicinity. (c) Rise (upper) and decay times (lower) of the green (left) and red (right) emission with the color code as in part (b). (d) Schematic of the tip-enhancement of a single UC nanoparticle. (e) UC emission spectra with retracted and approached tip, respectively. (f) Decay curves for red emission detected with and without tip at 660 nm[5, 40]

**Single particle multicolor barcoding** Optical microbarcodes are emerging as an attractive media for multiplexed analyte detection or anti-counterfeiting applications[41-47]. Here the lanthanide-doped UC system with multicolor Anti-Stokes emissions using single-wavelength NIR laser excitation provides a feasible strategy to generate a large, diverse library of optical barcodes. However, it is still a challenge to display an optical barcode in single particle level because of the optical resolution limitation of the common designed core-shell UC nanoparticles. Therefore, it is critical to design a multicolor structure with the monochromaticity of spatial separation. Recently, Liu *et al*. reported a design that one-dimensional epitaxial growth on the tips of a parent rod structure, where different activators exhibiting RGB colors were doped in the epitaxial material and parent rods, respectively (Figure 11 (a))[48]. Using the confocal single particle optical characterization, the energy transfer at the tip junction was investigated by lifetime comparison. The unaltered lifetimes of $Er^{3+}$ recorded at three different spots obtained with focus moving indicated that there is no apparent crosstalk between $Tm^{3+}$ and $Er^{3+}$ activators even at the tip junction.

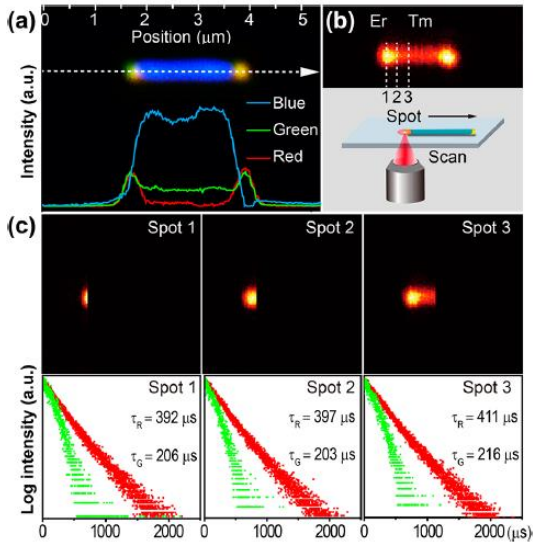


**Figure 12** (a) Wide-field luminescence image of a single microrod exhibiting YBY dual-color UC emission. (b) Confocal microscope image of a different dual-color microrod. (c) The corresponding green ($^4S_{3/2}$) and red ($^4F_{9/2}$) emission lifetimes in three different areas (marked with spot 1, 2, 3 shown in b) of the microrod[48]

Nanoscale

ARTICLE

## Conclusion and perspective

Significant achievements in the fields of UCNPs have been made in the past few years promptly, spanning from nanofabrication, photophysical theory, to application. Towards the further enormous progress, the advanced technical promotion in regards of the crystal growth kinetic related intrinsic structure combing with the size effect, surface effect, and local field effect is urgently necessary. In this regard, the characterization of single nanoparticle UC behaviors is extremely effective to offer breakthrough insight of the UC investigations. Beyond the universality of ensemble spectroscopy, single particle optical characterization exhibits its superiority in inhomogeneous or anisotropic spectra, unique photophysical phenomena, and tailored applications.

Despite the growing efforts have been devoted to the single particle behavior of UC luminescence, further thinking to push the research to a remarkable depth and breadth are necessary. Firstly, the major challenge for single nanoparticle characterization is centered on the sensitivity issue. The quantum efficiency of small size UCNPs is still low. The success of single particle detection mainly relies on the laser irradiation with high power density up to ~$10^6$ W·cm$^{-2}$. However, this high energy input at the focus point may causes side effect and even irreversible damage of the application environment in some cases. Meanwhile, in limitation of the UCNPs' brightness, the current investigations of single particles are mainly located in the species of $Er^{3+}$ and $Tm^{3+}$, which have efficient UC sensitized by $Yb^{3+}$. Therefore, the high quality UCNPs with high-technical nanofabrication is urgently pursued[49], and more effective way to collect the nondirectional emitting light is expected to improve the sensitivity. On the other hand, because there are no commercial instruments available with single nanoparticle sensitivity, only a few leading research groups with instrumentation expertise have such capability to purposely build instruments and carry out advanced optical characterizations of single UCNPs. More encouragements are needed for multidisciplinary research community to purposely build instruments to further advance this field. Secondly, the high speed nanopositioning function aiming at single particles with size of 1-100 nm in the optical detection technique is pursued. Taking the confocal scanning technique as an example, the specimen treatment and point-by-point scanning way is time consuming. Also it should be noticed that the less optical components employed in the detection part, the high credibility of the data collected and high signal-to-noise ratio will be achieved. Thirdly, systematic researches with precise controllability of optical-function in single nanoparticle level are expected to be carried out beyond the limits of current phenomenological exploration. For example, the accession of external fields on single UCNPs, *e.g.,* cryogenics, pressure, and magnetic or electronic fields, are expected to show fantastic modulation capability of UC luminescence. Up to now, we consider that the most promising applicable way out of UC luminescence from single nanoparticles lies in the optical super-resolution imaging and the dynamic detection of diagnosis and therapy in biomedical fields.

## Acknowledgements

The authors acknowledge financial support from Zhejiang Provincial Natural Science Foundation of China (No. LY14E020007) and National Natural Science Foundation of China (No. 11404311).

## References

1. X. Huang, S. Han, W. Huang and X. Liu, *Chem Soc Rev*, 2013, 42, 173-201.
2. F. Wang, R. R. Deng, J. Wang, Q. X. Wang, Y. Han, H. M. Zhu, X. Y. Chen and X. G. Liu, *Nat Mater*, 2011, 10, 968-973.
3. S. W. Wu, G. Han, D. J. Milliron, S. Aloni, V. Altoe, D. V. Talapin, B. E. Cohen and P. J. Schuck, *Proc Natl Acad Sci USA*, 2009, 106, 10917-10921.
4. S. Schietinger, L. D. Menezes, B. Lauritzen and O. Benson, *Nano Lett*, 2009, 9, 2477-2481.
5. S. Schietinger, T. Aichele, H. Q. Wang, T. Nann and O. Benson, *Nano Lett*, 2010, 10, 134-138.
6. J. J. Zhou, G. X. Chen, E. Wu, G. Bi, B. T. Wu, Y. Teng, S. F. Zhou and J. R. Qiu, *Nano Lett*, 2013, 13, 2241-2246.
7. D. J. Gargas, E. M. Chan, A. D. Ostrowski, S. Aloni, M. V. P. Altoe, E. S. Barnard, B. Sanii, J. J. Urban, D. J. Milliron, B. E. Cohen and P. J. Schuck, *Nat Nanotechnol*, 2014, 9, 300-305.
8. R. Kolesov, K. Xia, R. Reuter, R. Stohr, A. Zappe, J. Meijer, P. R. Hemmer and J. Wrachtrup, *Nat Commun*, 2012, 1029.
9. A. D. Ostrowski, E. M. Chan, D. J. Gargas, E. M. Katz, G. Han, P. J. Schuck, D. J. Milliron and B. E. Cohen, *ACS nano*, 2012, 6, 2686-2692.
10. S. C. Warren-Smith, S. Afshar and T. M. Monro, *Opt Express*, 2008, 16, 9034-9045.
11. S. V. Afshar, Y. L. Ruan, S. C. Warren-Smith and T. M. Monro, *Opt Lett*, 2008, 33, 1473-1475.
12. Y. Ruan, E. P. Schartner, H. Ebendorff-Heidepriem,

Hoffmann and T. M. Monro, *Opt Express*, 2007, 15, 17819-17826.
13. J. B. Zhao, D. Y. Jin, E. P. Schartner, Y. Q. Lu, Y. J. Liu, A. V. Zvyagin, L. X. Zhang, J. M. Dawes, P. Xi, J. A. Piper, E. M. Goldys and T. M. Monro, *Nat Nanotechnol*, 2013, 8, 729-734.
14. E. P. Schartner, D. Y. Jin, H. Ebendorff-Heidepriem, J. A. Piper, Z. D. Lu and T. M. Monro, *Nanoscale*, 2012, 4, 7448-7451.
15. R. M. Dickson, A. B. Cubitt, R. Y. Tsien and W. E. Moerner, *Nature*, 1997, 388, 355-358.
16. M. Nirmal, B. Dabbousi, M. Bawendi, J. Macklin, J. Trautman, T. Harris and L. Brus, *Nature*, 1996, 383, 802-804.
17. C. Galland, Y. Ghosh, A. Steinbruck, M. Sykora, J. A. Hollingsworth, V. I. Klimov and H. Htoon, *Nature*, 2011, 479, 203-207.
18. M. Barnes, A. Mehta, T. Thundat, R. Bhargava, V. Chhabra and B. Kulkarni, *J Phys Chem B*, 2000, 104, 6099-6102.
19. Y. I. Park, J. H. Kim, K. T. Lee, K. S. Jeon, H. Bin Na, J. H. Yu, H. M. Kim, N. Lee, S. H. Choi, S. I. Baik, H. Kim, S. P. Park, B. J. Park, Y. W. Kim, S. H. Lee, S. Y. Yoon, I. C. Song, W. K. Moon, Y. D. Suh and T. Hyeon, *Adv Mater*, 2009, 21, 4467-4471.
20. X. M. Li, R. Wang, F. Zhang and D. Y. Zhao, *Nano Lett*, 2014, 14, 3634-3639.
21. G. Mialon, S. Turkcan, G. Dantelle, D. P. Collins, M. Hadjipanayi, R. A. Taylor, T. Gacoin, A. Alexandrou and J. P. Boilott, *J Phys Chem C*, 2010, 114, 22449-22454.
22. F. Zhang, Q. H. Shi, Y. C. Zhang, Y. F. Shi, K. L. Ding, D. Y. Zhao and G. D. Stucky, *Adv Mater*, 2011, 23, 3775-+.
23. L. Zhou, R. Wang, C. Yao, X. Li, C. Wang, X. Zhang, C. Xu, A. Zeng, D. Zhao and F. Zhang, *Nat Commun*, 2015, 6, 6938.
24. P. Chen, M. Song, E. Wu, B. Wu, J. Zhou, H. Zeng, X. Liu and J. Qiu, *Nanoscale*, 2015, DOI: DOI: 10.1039/c5nr00289c.
25. J. Wang, R. Deng, M. A. MacDonald, B. Chen, J. Yuan, F. Wang, D. Chi, T. S. Hor, P. Zhang, G. Liu, Y. Han and X. Liu, *Nat Mater*, 2014, 13, 157-162.
26. F. Wang and X. G. Liu, *J Am Chem Soc*, 2008, 130, 5642-5643.
27. H. Zhang, Y. Li, Y. Lin, Y. Huang and X. Duan, *Nanoscale*, 2011, 3, 963-966.
28. A. Yin, Y. Zhang, L. Sun and C. Yan, *Nanoscale*, 2010, 2, 953-959.
29. V. Mahalingam, F. Vetrone, R. Naccache, A. Speghini and J. A. Capobianco, *Adv Mater*, 2009, 21, 4025-4028.
30. K. W. Krämer, D. Biner, G. Frei, H. U. Güdel, M. P. Hehlen and S. R. Lüthi, *Chem Mater*, 2004, 16, 1244-1251.
31. L. Liang, H. Wu, H. Hu, M. Wu and Q. Su, *J Alloy Compd*, 2004, 368, 94-100.
32. M. Nyk, R. Kumar, T. Y. Ohulchanskyy, E. J. Bergey and P. N. Prasad, *Nano Lett*, 2008, 8, 3834-3838.
33. J. J. Zhou, G. X. Chen, Y. B. Zhu, L. L. Huo, W. Mao, D. N. Zou, X. W. Sun, E. Wu, H. P. Zeng, J. J. Zhang, L. Zhang, J. R. Qiu and S. Q. Xu, *J Mater Chem C*, 201[illegible] 3, 364-369.
34. Y. Q. Lu, J. B. Zhao, R. Zhang, Y. J. Liu, D. M. Liu, E. M[illegible] Goldys, X. S. Yang, P. Xi, A. Sunna, J. Lu, Y. Shi, R. C[illegible] Leif, Y. J. Huo, J. Shen, J. A. Piper, J. P. Robinson and [illegible] D. Y. Jin, *Nat Photonics*, 2014, 8, 33-37.
35. R. Kolesov, R. Reuter, K. W. Xia, R. Stohr, A. Zappe and [illegible] Wrachtrup, *Phys Rev B*, 2011, 84.
36. A. M. Glass, P. F. Liao, J. G. Bergman and D. H. Olson, *Opt Lett*, 1980, 5, 368-370.
37. J. R. Lakowicz, *Analytical biochemistry*, 2001, 298, 1-24.
38. E. Dulkeith, A. C. Morteani, T. Niedereichholz, T. A. Klar, J. Feldmann, S. A. Levi, F. C. van Veggel, D. N. Reinhoudt, M. Moller and D. I. Gittins, *Phys Rev Lett*, 2002, 89, 203002.
39. M. Saboktakin, X. Ye, S. J. Oh, S. H. Hong, A. T. Fafarman, U. K. Chettiar, N. Engheta, C. B. Murray and C. [illegible] Kagan, *ACS nano*, 2012, 6, 8758-8766.
40. N. Mauser, D. Piatkowski, T. Mancabelli, M. Nyk, S. Mackowski and A. Hartschuh, *ACS nano*, 2015.
41. J. M. Nam, C. S. Thaxton and C. A. Mirkin, *Science*, 2003, 301, 1884-1886.
42. S. S. Agasti, M. Liong, V. M. Peterson, H. Lee and R. Weissleder, *J Am Chem Soc*, 2012, 134, 18499-18502.
43. S. H. Kim, J. W. Shim and S. M. Yang, *Angew Chem Int Ed*, 2011, 50, 1171-1174.
44. D. C. Pregibon, M. Toner and P. S. Doyle, *Science*, 2007, 315, 1393-1396.
45. B. Creran, B. Yan, D. F. Moyano, M. M. Gilbert, R. W. Vachet and V. M. Rotello, *Chem Commun*, 2012, 48, 4543-4545.
46. M. J. Dejneka, A. Streltsov, S. Pal, A. G. Frutos, C. L. Powell, K. Yost, P. K. Yuen, U. Muller and J. Lahiri, *Proc Natl Acad Sci USA*, 2003, 100, 389-393.
47. H. H. Gorris and O. S. Wolfbeis, *Angew Chem Int Ed*, 2013, 52, 3584-3600.
48. Y. H. Zhang, L. X. Zhang, R. R. Deng, J. Tian, Y. Zong, D. Jin and X. G. Liu, *J Am Chem Soc*, 2014, 136, 4893-4896.
49. M. L. Deng and L. Y. Wang, *Nano Res*, 2014, 7, 782-793.